Communication

Operando Observation of Oxygenated Intermediates during CO Hydrogenation on Rh Single Crystals

David Degerman,* Mikhail Shipilin, Patrick Lömker, Christopher M. Goodwin, Sabrina M. Gericke, Uta Hejral, Jörgen Gladh, Hsin-Yi Wang, Christoph Schlueter, Anders Nilsson, and Peter Amann

Read Online

ACCESS | Metrics & More | Article Recommendations | Supporting Information

ABSTRACT: The CO hydrogenation reaction over the Rh(111) and (211) surfaces has been investigated operando by X-ray photoelectron spectroscopy at a pressure of 150 mbar. Observations of the resting state of the catalyst give mechanistic insight into the selectivity of Rh for generating ethanol from CO hydrogenation. This study shows that the Rh(111) surface does not dissociate all CO molecules before hydrogenation of the O and C atoms, which allows methoxy and other both oxygenated and hydrogenated species to be visible in the photoelectron spectra.

The mixture of CO, CO_2, and H_2, known as synthesis gas or syngas, can be used to produce chemicals and fuels.[1,2] New approaches utilizing biomass production, hydrogen from water splitting, and direct capture of atmospheric CO_2 have opened up the possibility for sustainable manufacturing routes, lowering the dependence on fossil resources.[2−5]

These processes rely on active and selective catalysts where the selectivity toward multicarbon oxygenates (referred to as C2+ oxygenates) is desired, as they have a high volumetric and gravimetric energy density and contain functional groups.[1] Rhodium is a catalyst that has a slightly elevated selectivity toward C2+ oxygenates in general and higher alcohols in particular in comparison to other metals.[1,6,7] The reason for the high C2+ oxygenates selectivity could be that CO adsorb onto the Rh surface both dissociatively and nondissociatively. Hydrogen atoms will sequentially attach to the C and O species to form CH_4 and H_2O. Before the attachment of a final hydrogen atom, however, there is a probability that the CH_x species will bind to CO rather than H and form a CH_xCO intermediate.[6−11] The bond formation between unsaturated hydrocarbons and nondissociated CO is proposed to be the crucial step when creating multicarbon oxygenates.

Theoretical calculations of reaction barriers significantly contributed to the proposed oxygenates mechanism. Calculated values for the ground-state and transition-state energies for every intermediate have been combined into a microkinetic model (MKM). The predicted turnover frequencies (TOFs) have been compared to experimental TOFs with relatively good agreement.[12−14] The coverages of adsorbates depict the catalyst's resting state, i.e., species at the minima of the potential energy surface, and provide a more direct correlation to the reaction mechanism than the TOFs of various products. In the past, experimental difficulties have prevented this determination, because it requires a combination of (1) surface sensitivity, (2) element and compound specificity, and (3) operando conditions. X-ray photoelectron spectroscopy (XPS) fulfills the first two criteria but has been very impractical to perform operando during hydrogenation reactions because of

the necessity of high pressures. XPS studies of Rh and other syngas catalysts have consequently been limited to pressures around or below 0.2 mbar.[15−17] With recent advances in XPS instrumentation and the virtual pressure cell concept, we now have the experimental tools to examine reaction conditions at pressures in the hundreds of mbar regime.[18]

We have probed the CO and CO_2 hydrogenation reactions over Rh(111) and Rh(211) by XPS at a pressure of 150 mbar and report herein the observation of oxygenate intermediates in line with the reaction pathway expected by DFT calculations.[14] For fcc metallic systems such as Rh, the (111) surface comprises a flat terrace of close-packed atoms and the (211) surface has a high step density.[6,13] Comparing the two surface orientations assists in elucidating the effect of undercoordinated step edges, which are known to impact the rate of dissociation for bonds such as the C≡O bond of a CO_2 molecule.[10,19,20] This comparison is important because the feasibility of CO and CO_2 bond breaking on Rh(111) has been debated.[21−25]

Figure 1 shows X-ray photoelectron (XP) spectra of the C 1s region during CO hydrogenation on Rh(111) and Rh(211). The spectrum intensity, which is proportional to the surface coverage, was estimated for all spectra. The total carbon coverage on Rh(111) decreases with temperature from 96% of a monolayer (ML) at 175 °C down to 12% of an ML at 325 °C. Similarly, on Rh(211), the coverage ranges from 80.5% of an ML down to 11% in the same temperature span. The recoil of the high-energy photoelectrons and coadsorption effects may cause the peak positions to be slightly different from more conventional soft X-ray experiments.[26−29] For a detailed
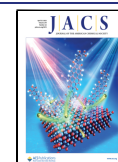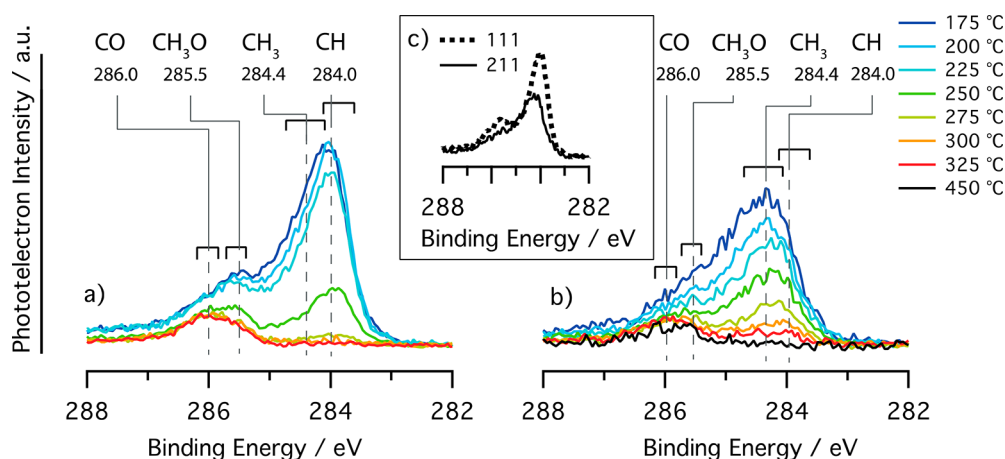
Figure 1. XP spectra acquired during CO hydrogenation of the C 1s region for two different Rh surfaces: (a) the (111) surface and (b) the (211) surface; (c) comparison of the 200 °C spectra for both surfaces. The CO:H$_2$ ratio was 1:2, the photon energy was 4.6 keV, and the pressure was 150 mbar. A full description of the experimental parameters is available in the Supporting Information.

technical discussion on the spectra, we refer to the Supporting Information.

Four components are identified in Figure 1. The first two are the global peak maxima at the lowest temperatures, 175−200 °C, which on the (111) surface is found at 284.0 eV binding energy (BE), and on the (211) surface, it is located at 284.4 eV. These peaks correspond to differently hydrogenated CH$_x$ fragments. We attribute the 284.0 eV peak to CH and the 284.4 eV peak to CH$_3$. Other species that contribute to the spectrum intensity include atomic C, CH$_2$, and C−C bonded carbon.[29,30] The coverage of the hydrocarbon species decreases with increasing temperature, which is likely an effect of faster termination of the hydrocarbon intermediates resulting in higher reaction rates.[31]

At 275−325 °C, we observe a peak at 286.0 eV for both surface orientations related to CO in the on-top position, the energetically most favorable site.[32] The CO coverage, as seen in Figure 2, is stable at around 7−10% of an ML on Rh(111) and 6−8% of an ML on Rh(211).

Lastly, the second maximum is a peak located at 285.5 eV, and most visible at temperatures 175−250 °C on the Rh(111) surface. It is well-known that CO in hollow sites has lower

binding energy than CO on-top-site. It is, however, very unlikely that those sites become populated to a large degree at coverages lower than 33% of a ML.[32,33] Thus, we denote the peak at 285.5 eV as the methoxy (CH$_3$O) intermediate. Other oxygenated products such as ethoxy (CH$_3$CH$_2$O), may contribute as well. The methoxy species is more prevalent on the (111) surface than on the (211) surface, consistent with the expectedly slower CO dissociation on the (111) surface. The CO and methoxy species are further confirmed by the O 1s spectra provided in the Supporting Information. Some hydrocarbon fragments in the 284−284.5 region can be related to the formation of C2+ oxygenates but we cannot firmly conclude that in the XP spectra because of overlap with their monocarbon equivalents.

In Figure 2, we have plotted how the coverages of the four fitted components change with temperature. We note a decrease of all components with temperature except for the 286.0 eV peak, which corresponds to CO. We have minor indications of hydrocarbon and methanol formation in the online mass spectrometry (MS) acquisition provided in the Supporting Information.

XP spectra of the C 1s region during CO$_2$ hydrogenation are shown in Figure 3. We can discern two main peaks, one corresponding to CH$_x$ at 284.0 eV and a second peak corresponding to oxygenated C species around 286.0 eV. Qualitatively, the same types of surface species are present in the CO$_2$ hydrogenation reaction as for CO hydrogenation, but with significantly lower coverages. The total coverage of carbon species on both Rh(111) and Rh(211) are between 2 and 10% of an ML. The lower coverage for the CO$_2$ hydrogenation reaction can be clearly seen in Figure 3c, where the adsorbate spectra of the two reactions are compared. The weak binding of CO$_2$ to Rh results in a short residence time on the surface and, in turn, low probability for CO$_2$ dissociation.[17] The higher coverage of the (211) surface compared to the (111) surface is expected because the dissociation rates of CO$_2$ have been estimated to be faster because of lower barriers on the (211) surface.[34,35]
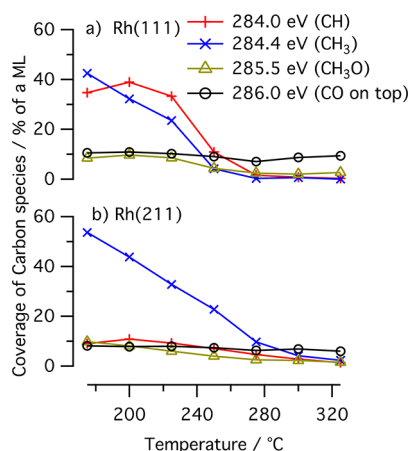

Figure 2. Trends in coverages of chemisorbed carbon-containing species during CO hydrogenation as obtained by fitting of the spectra in Figure 1. Results for (a) Rh(111) and (b) Rh(211). The fits are available in the Supporting Information.

◼ IMPLICATIONS OF RESULTS

The presence of methoxy species (or other oxygenates) indicates that some CO is almost fully hydrogenated before dissociation. The fact that the coverage of CH$_x$ species is
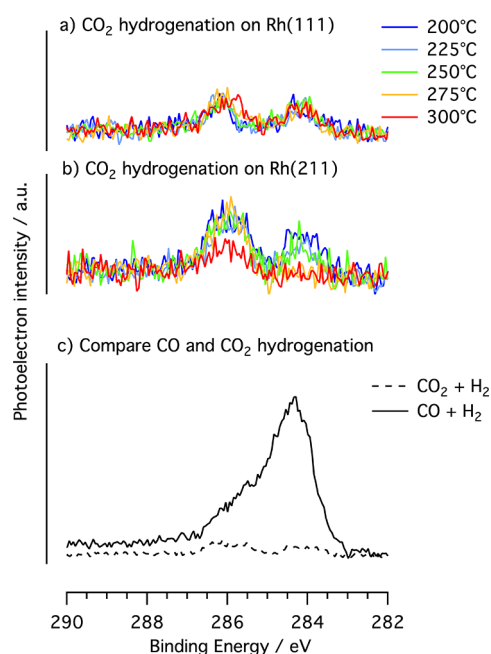
Figure 3. XP spectra of the C 1s region during CO_2 hydrogenation on (a) Rh(111) and (b) Rh(211). (c) Comparison of the spectra acquired during CO and CO_2 hydrogenation on Rh(211) at $T = 200$ °C. The pressure in all spectra is 150 mbar and the $CO_2/CO:H_2$ ratio is 1:2.

temperature dependent tells us that other CO molecules are actively dissociated in the presence of H_2. This holds for both the stepped (211) surface and the more terrace-like (111) surface. These observations support the hypothesis that CO is hydrogenated both before and after dissociation on Rh and is consistent with DFT calculations proposing that the hydrogen-assisted dissociation step occurs via the CH_3O intermediate.[14] The observation of CH_3O may also be indicative of methanol production, consistent with the MS data in the Supporting Information.

Theoretical calculations have indicated that the Rh(111) surface likely has higher selectivity than the (211) surface toward C2+ oxygenates. The reasoning is related to the higher activity for the competing methanation reaction on the (211) surface, whereas C−C coupling reactions require a coexistence of nondissociated CO and nonsaturated CH_x-species, and it has been shown that the rate for C−C coupling increase with increasing CO coverage.[11,13] The dominance of CH_x species in Figure 1 below 250 °C on both surface orientations indicate a low-CO-coverage regime which favors monocarbon products. Still, it is interesting to examine the prerequisites for C−C coupling of the examined reaction conditions. We note a higher degree of hydrogen saturation on the (211) surface, whereas the (111) surface at lower temperatures has a higher fraction covered in low-saturated hydrocarbons. DFT studies have shown that CO insertion into CH is has lower barriers than insertion into CH_3.[6,36] Both CO and CH_x show in general higher coverage on the (111) surface. Additionally, a resting state of mainly CH means less immediate competition from the termination reaction producing hydrocarbons. These observations combined lead us to conclude that the prerequisites for C−C coupling are favorable on the (111) surface around 250 °C or below.

The CO coverage dependence could be one of the reasons high pressure is needed to obtain more C−C coupling in CO

hydrogenation. Another factor that has been debated is the coadsorption with H_2. Low energy electron diffraction and electron energy loss spectroscopy studies of CO on Rh(111) have shown that the coverage is unaffected by the coadsorption of H_2.[37] Several of the DFT studies utilize this assumption in their theoretical calculations.[6,13,38] In stark contrast, temperature-programmed desorption studies in ultrahigh vacuum of the same system have shown that the uptake of CO on Rh(111) is heavily dependent on the presence of H_2 and that the CO coverage saturates at ∼15% of a ML hydrogen for precovered surfaces.[39] This work supports a picture where coadsorbed H severely limits the uptake of CO on Rh surfaces, based on the following observations: We note on Rh(111) a CO-on-top coverage of 7−10% that does not decrease significantly with increasing temperature up to 325 °C. In the case of dynamic equilibrium, we would have expected the coverage to decrease with increasing temperature as the desorption rate of CO is strongly temperature dependent. Still, we only see this effect in Figure 1b, where the CO-on-top region is slightly diminished at 450 °C (see also Figure S9 in the Supporting Information). For all other temperatures, on both the (111) and (211) surfaces, we note a relatively stable coverage and consequently conclude that the CO must be at saturation coverage. At temperatures below 250 °C, the coadsorption with other carbon species will prevent the CO species from covering the surface, which may cause the CO coverage to saturate, but even above 275 °C, where CO is the only spectroscopically visible C 1s species, we observe the 7−10% coverage. We thus propose that the spectroscopically nonvisible hydrogen competes with CO for adsorption sites and causes the CO to saturate.

In conclusion, we have utilized operando XPS during CO and CO_2 hydrogenation reactions on Rh(211) and Rh(111) catalysts for a mechanistic investigation. The surface adsorbates comprise mainly CO, hydrocarbons and methoxy radicals. We have found indications that the CO coverage is heavily affected by the coadsorption of $H_{(ads)}$. The degree of hydrogenation is sensitive to the surface orientation, and the coverage of hydrocarbons and methoxy is temperature dependent. For the prospect of production of C2+ oxygenates, such as ethanol, a higher partial pressure of CO is required to increase the C−C coupling rate. In the currently studied reaction conditions the Rh(111) surface around 225−250 °C has better prerequisites for C−C coupling than the other studied conditions. In the CO_2 hydrogenation reaction, we observe CO and unsaturated hydrocarbons, but at much lower coverages. In general, we conclude that insights of the presence of different adsorbates during operando studies assists in understanding selectivity in syngas reactions.

■ ASSOCIATED CONTENT

ⓈI Supporting Information

The Supporting Information is available free of charge at https://pubs.acs.org/doi/10.1021/jacs.2c00300.

> Detailed description of materials and methods, O 1s and Rh 3d spectra, fitted C 1s spectra, technical discussion of spectra and peak assignment, mass spectrometry data, and discussion (PDF)

◼ AUTHOR INFORMATION

Corresponding Author

David Degerman — *Department of Physics, AlbaNova University Center, Stockholm University, Stockholm 114 21, Sweden;* ⦿ orcid.org/0000-0001-6085-2916; Email: david.degerman@fysik.su.se

Authors

Mikhail Shipilin — *Department of Physics, AlbaNova University Center, Stockholm University, Stockholm 114 21, Sweden*

Patrick Lömker — *Department of Physics, AlbaNova University Center, Stockholm University, Stockholm 114 21, Sweden*

Christopher M. Goodwin — *Department of Physics, AlbaNova University Center, Stockholm University, Stockholm 114 21, Sweden*

Sabrina M. Gericke — *Department of Physics Combustion Physics, Lund University, Lund 223 63, Sweden*

Uta Hejral — *Division of Synchrotron Radiation Research, Lund University, Lund 223 63, Sweden*

Jörgen Gladh — *Department of Physics, AlbaNova University Center, Stockholm University, Stockholm 114 21, Sweden;* ⦿ orcid.org/0000-0002-5389-5675

Hsin-Yi Wang — *Department of Physics, AlbaNova University Center, Stockholm University, Stockholm 114 21, Sweden*

Christoph Schlueter — *Photon Science, Deutches Elektronen Synchrotron DESY, Hamburg 226 07, Germany*

Anders Nilsson — *Department of Physics, AlbaNova University Center, Stockholm University, Stockholm 114 21, Sweden;* ⦿ orcid.org/0000-0003-1968-8696

Peter Amann — *Department of Physics, AlbaNova University Center, Stockholm University, Stockholm 114 21, Sweden*

Complete contact information is available at:
https://pubs.acs.org/10.1021/jacs.2c00300

Author Contributions

The manuscript was written through contributions of all authors and all authors have given approval to the final version of the manuscript.

Notes

The authors declare no competing financial interest.

◼ ABBREVIATIONS

DFT, density functional theory
MKM, microkinetic model
TOF, turnover frequency
XPS, X-ray photoelectron spectroscopy
XP, X-ray photoelectron
ML, monolayer
MS, mass spectrometry

◼ REFERENCES

(1) Luk, H. T.; Mondelli, C.; Ferré, D. C.; Stewart, J. A.; Pérez-Ramírez, J. Status and Prospects in Higher Alcohols Synthesis from Syngas. *Chem. Soc. Rev.* **2017**, *46* (5), 1358−1426.

(2) *Hydrogen and Syngas Production and Purification Technologies*; Liu, K., Song, C., Subramani, V., Eds.; John Wiley & Sons: Hoboken, NJ, 2010; Vol. *2010*.

(3) Yang, H.; Xu, Z.; Fan, M.; Gupta, R.; Slimane, R. B.; Bland, A. E.; Wright, I. Progress in Carbon Dioxide Separation and Capture: A Review. *J. Environ. Sci.* **2008**, *20* (1), 14−27.

(4) Munasinghe, P. C.; Khanal, S. K. Biomass-Derived Syngas Fermentation into Biofuels. *Biofuels* **2011**, *101* (13), 79−98.

(5) Ahmad, H.; Kamarudin, S. K.; Minggu, L. J.; Kassim, M. Hydrogen from Photo-Catalytic Water Splitting Process: A Review. *Renew. Sustain. Energy Rev.* **2015**, *43*, 599−610.

(6) Yang, N.; Medford, A. J.; Liu, X.; Studt, F.; Bligaard, T.; Bent, S. F.; Nørskov, J. K. Intrinsic Selectivity and Structure Sensitivity of Rhodium Catalysts for C2 + Oxygenate Production. *J. Am. Chem. Soc.* **2016**, *138* (11), 3705−3714.

(7) Wang, J.; Liu, Z.; Zhang, R.; Wang, B. Ethanol Synthesis from Syngas on the Stepped Rh(211) Surface: Effect of Surface Structure and Composition. *J. Phys. Chem. C* **2014**, *118* (39), 22691−22701.

(8) Gu, T.; Wang, B.; Chen, S.; Yang, B. Automated Generation and Analysis of the Complex Catalytic Reaction Network of Ethanol Synthesis from Syngas on Rh(111). *ACS Catal.* **2020**, *10* (11), 6346−6355.

(9) Mei, D.; Rousseau, R.; Kathmann, S. M.; Glezakou, V. A.; Engelhard, M. H.; Jiang, W.; Wang, C.; Gerber, M. A.; White, J. F.; Stevens, D. J. Ethanol Synthesis from Syngas over Rh-Based/SiO2 Catalysts: A Combined Experimental and Theoretical Modeling Study. *J. Catal.* **2010**, *271* (2), 325−342.

(10) Filot, I. A. W.; Broos, R. J. P.; Van Rijn, J. P. M.; Van Heugten, G. J. H. A.; Van Santen, R. A.; Hensen, E. J. M. First-Principles-Based Microkinetics Simulations of Synthesis Gas Conversion on a Stepped Rhodium Surface. *ACS Catal.* **2015**, *5* (9), 5453−5467.

(11) Schumann, M.; Nielsen, M. R.; Smitshuysen, T. E. L.; Hansen, T. W.; Damsgaard, C. D.; Yang, A. C. A.; Cargnello, M.; Grunwaldt, J. D.; Jensen, A. D.; Christensen, J. M. Rationalizing an Unexpected Structure Sensitivity in Heterogeneous Catalysis-CO Hydrogenation over Rh as a Case Study. *ACS Catal.* **2021**, *11* (9), 5189−5201.

(12) Medford, A. J.; Vojvodic, A.; Hummelshøj, J. S.; Voss, J.; Abild-Pedersen, F.; Studt, F.; Bligaard, T.; Nilsson, A.; Nørskov, J. K. From the Sabatier Principle to a Predictive Theory of Transition-Metal Heterogeneous Catalysis. *J. Catal.* **2015**, *328*, 36−42.

(13) Schumann, J.; Medford, A. J.; Yoo, J. S.; Zhao, Z.-J.; Bothra, P.; Cao, A.; Studt, F.; Abild-Pedersen, F.; Nørskov, J. K. Selectivity of Synthesis Gas Conversion to C 2+ Oxygenates on Fcc(111) Transition-Metal Surfaces. *ACS Catal.* **2018**, *8* (4), 3447−3453.

(14) Choi, Y. M.; Liu, P. Mechanism of Ethanol Synthesis from Syngas on Rh(111). *J. Am. Chem. Soc.* **2009**, *131* (36), 13054−13061.

(15) Martin, N. M.; Hemmingsson, F.; Schaefer, A.; Ek, M.; Merte, L. R.; Hejral, U.; Gustafson, J.; Skoglundh, M.; Dippel, A. C.; Gutowski, O.; Bauer, M.; Carlsson, P. A. Structure-Function Relationship for CO2 Methanation over Ceria Supported Rh and

Ni Catalysts under Atmospheric Pressure Conditions. *Catal. Sci. Technol.* **2019**, *9* (7), 1644−1653.

(16) Schnadt, J.; Knudsen, J.; Johansson, N. Present and New Frontiers in Materials Research by Ambient Pressure X-Ray Photoelectron Spectroscopy. *J. Phys.: Condens. Matter* **2020**, *32* (41), 413003.

(17) Kim, J.; Ha, H.; Doh, W. H.; Ueda, K.; Mase, K.; Kondoh, H.; Mun, B. S.; Kim, H. Y.; Park, J. Y. How Rh Surface Breaks CO_2 Molecules under Ambient Pressure. *Nat. Commun.* **2020**, *11* (1), 5649.

(18) Amann, P.; Degerman, D.; Lee, M. T.; Alexander, J. D.; Shipilin, M.; Wang, H. Y.; Cavalca, F.; Weston, M.; Gladh, J.; Blom, M.; Björkhage, M.; Löfgren, P.; Schlueter, C.; Loemker, P.; Ederer, K.; Drube, W.; Noei, H.; Zehetner, J.; Wentzel, H.; Åhlund, J.; Nilsson, A. A High-Pressure x-Ray Photoelectron Spectroscopy Instrument for Studies of Industrially Relevant Catalytic Reactions at Pressures of Several Bars. *Rev. Sci. Instrum.* **2019**, *90* (10), 103102.

(19) Dahl, S.; Logadottir, A.; Egeberg, R. C.; Larsen, J. H.; Chorkendorff, I.; Törnqvist, E.; Nørskov, J. K. Role of Steps in N2 Activation on Ru(0001). *Phys. Rev. Lett.* **1999**, *83* (9), 1814−1817.

(20) Mavrikakis, M.; Bäumer, M.; Freund, H.-J.; Norskov, J. K. Structure Sensitivity of CO Dissociation on Rh Surfaces. *Catal. Lett.* **2002**, *81* (3−4), 153−156.

(21) Yates, J. T.; Williams, E. D.; Weinberg, W. H. Does Chemisorbed Carbon Monoxide Dissociate on Rhodium? *Surf. Sci.* **1980**, *91* (2−3), 562−570.

(22) Ren, D. M.; Liu, W. A Study of Chemisorption Behavior of Carbon Monoxide on Rhodium Surfaces. *Surf. Sci.* **1990**, *232* (3), 316−322.

(23) Goodman, D. W.; Peebles, D. E.; White, J. M. CO2 Dissociation on Rhodium: Measurement of the Specific Rates on Rh(111). *Surf. Sci.* **1984**, *140* (1), L239−L243.

(24) Dubois, L. H.; Somorjai, G. A. The Dissociative Chemisorption of Carbon Dioxide on Rhodium Surfaces. *Surf. Sci.* **1979**, *88* (1), L13−L17.

(25) Kim, J.; Ha, H.; Doh, W. H.; Ueda, K.; Mase, K.; Kondoh, H.; Mun, B. S.; Kim, H. Y.; Park, J. Y. How Rh Surface Breaks CO 2 Molecules under Ambient Pressure. *Nat. Commun.* **2020**, *11*, 5649.

(26) Vesselli, E.; Baraldi, A.; Comelli, G.; Lizzit, S.; Rosei, R. Ethanol Decomposition: C-C Cleavage Selectivity on Rh(111). *ChemPhysChem* **2004**, *5* (8), 1133−1140.

(27) Solymosi, F. Thermal Stability and Reactions of CH2, CH3and C2H5species on the Metal Surfaces. *Catal. Today* **1996**, *28* (3), 193−203.

(28) Klivényi, G.; Solymosi, F. Generation of CH2 Species: Thermal and Photo-Induced Dissociation of CH2I2 on Rh(111) Surface. *Surf. Sci.* **1995**, *342* (1−3), 168−184.

(29) Yang, M. M.; Bao, X. H.; Li, W. X. Density Functional Theory Study of CHx (X = 1−3) Adsorption on Clean and CO Precovered Rh(111) Surfaces. *J. Chem. Phys.* **2007**, *127* (2), 024705.

(30) Bunnik, B. S.; Kramer, G. J. Energetics of Methane Dissociative Adsorption on Rh{111} from DFT Calculations. *J. Catal.* **2006**, *242* (2), 309−318.

(31) Saeidi, S.; Najari, S.; Fazlollahi, F.; Nikoo, M. K.; Sefidkon, F.; Klemeš, J. J.; Baxter, L. L. Mechanisms and Kinetics of CO2 Hydrogenation to Value-Added Products: A Detailed Review on Current Status and Future Trends. *Renew. Sustain. Energy Rev.* **2017**, *80* (June), 1292−1311.

(32) Smedh, M.; Beutler, A.; Ramsvik, T.; Nyholm, R.; Borg, M.; Andersen, J. N.; Duschek, R.; Sock, M.; Netzer, F. P.; Ramsey, M. G. Vibrationally Resolved C 1s Photoemission from CO Absorbed on Rh(111): The Investigation of a New Chemically Shifted C 1s Component. *Surf. Sci.* **2001**, *491* (1), 99−114.

(33) Payne, S. H.; Kreuzer, H. J.; Petenlinz, K. A.; Curtiss, T. J.; Uebing, C.; Sibener, S. J. Coverage Dependent Desorption Kinetics of CO from Rh(111): A Theoretical Analysis. *Surf. Sci.* **1992**, *272* (1−3), 102−110.

(34) Jiang, T.; Mowbray, D. J.; Dobrin, S.; Falsig, H.; Hvolbœk, B.; Bligaard, T.; Nørskov, J. K. Trends in CO Oxidation Rates for Metal

Nanoparticles and Close-Packed, Stepped, and Kinked Surfaces. *J. Phys. Chem. C* **2009**, *113* (24), 10548−10553.

(35) Falsig, H.; Hvolbæk, B.; Kristensen, I. S.; Jiang, T.; Bligaard, T.; Christensen, C. H.; Nørskov, J. K. Trends in the Catalytic CO Oxidation Activity of Nanoparticles. *Angew. Chemie - Int. Ed.* **2008**, *47* (26), 4835−4839.

(36) Zhao, Y. H.; Sun, K.; Ma, X.; Liu, J.; Sun, D.; Su, H. Y.; Li, W. X. Carbon Chain Growth by Formyl Insertion on Rhodium and Cobalt Catalysts in Syngas Conversion. *Angew. Chemie - Int. Ed.* **2011**, *50* (23), 5335−5338.

(37) Dubois, L. H.; Somorjai, G. A. The Chemisorption of CO and CO2 on Rh(111) Studied by High Resolution Electron Energy Loss Spectroscopy. *Surf. Sci.* **1980**, *91* (2−3), 514−532.

(38) Wang, S.; Petzold, V.; Tripkovic, V.; Kleis, J.; Howalt, J. G.; Skúlason, E.; Fernández, E. M.; Hvolbæk, B.; Jones, G.; Toftelund, A.; Falsig, H.; Björketun, M.; Studt, F.; Abild-Pedersen, F.; Rossmeisl, J.; Nørskov, J. K.; Bligaard, T. Universal Transition State Scaling Relations for (de)Hydrogenation over Transition Metals. *Phys. Chem. Chem. Phys.* **2011**, *13* (46), 20760.

(39) Williams, E. D.; Thiel, P. A.; Weinberg, W. H.; Yates, J. T. Segregation of Co-Adsorbed Species: Hydrogen and Carbon Monoxide on the (111) Surface of Rhodium. *J. Chem. Phys.* **1980**, *72* (6), 3496−3505.